UrbanMetaMapping-Transfer meeting

13-14/1/2025

Anastasios L. Kesidis, Kleomenis Kalogeropoulos

Department of Surveying and Geoinformatics Engineering
University of West Attica
Athens, Greece

Buildings extraction from historical topographic maps

Buildings extraction from historical topographic maps

- Geometric features extraction from historical maps

Input

Desired output

Extract the **buildings** from a sub-area patch of the original historical map

Buildings extraction from historical topographic maps

➢ Challenges

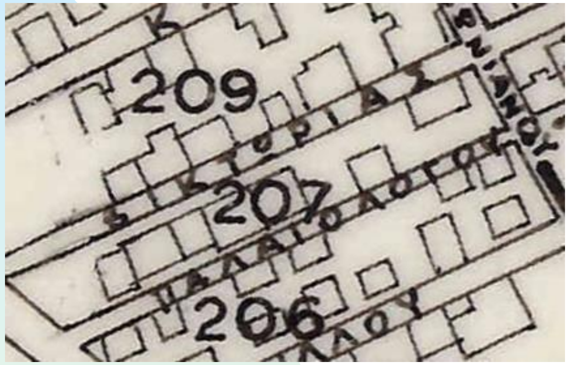

(a)

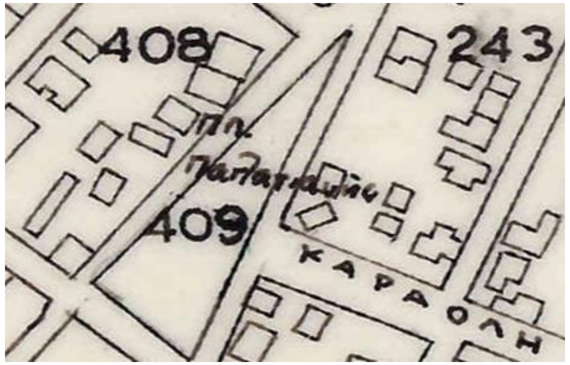

(b)

(c)

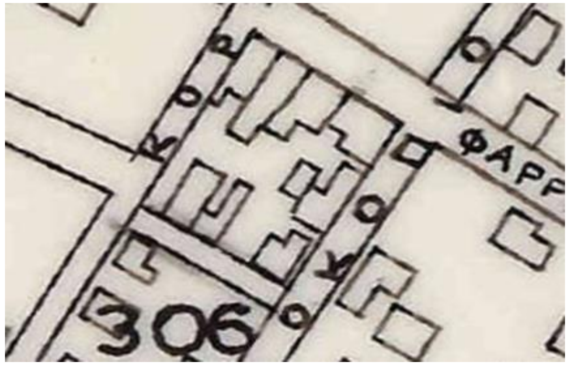

(d)

(a) Dense **text overlapping** content

(b) **Free text** over the map

(c) Buildings footprints with **varying shape, size and orientation**

(d) Overlapping issues between building **blocks** and building **footprints**

Buildings extraction from historical topographic maps

- Train a Deep Convolutional Neural Network (DCNN)

Patch of colored topographic map

Input

U-Net

Output

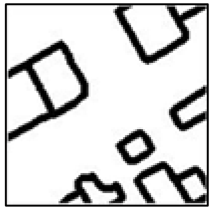

Patch of ground truth binary image denoting building footprints

- Patch sampling approaches

Random

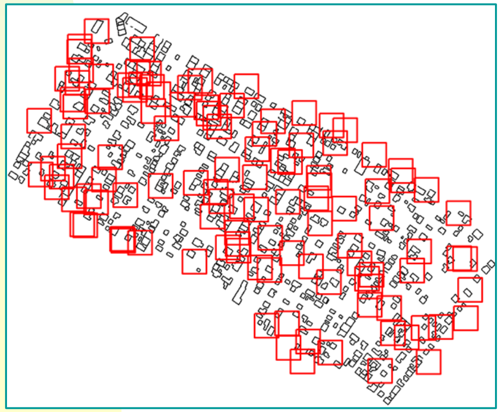

Grid based

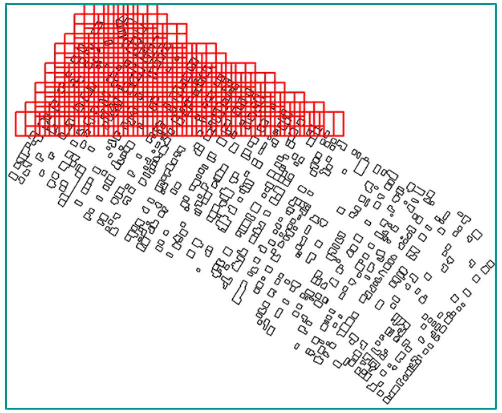

Buildings extraction from historical topographic maps

➢ Building **boundaries**

- Patch **size**: 64×64, 128×128 and 224×224
- Patch **sampling**: Random and Grid

224x224
"Random"

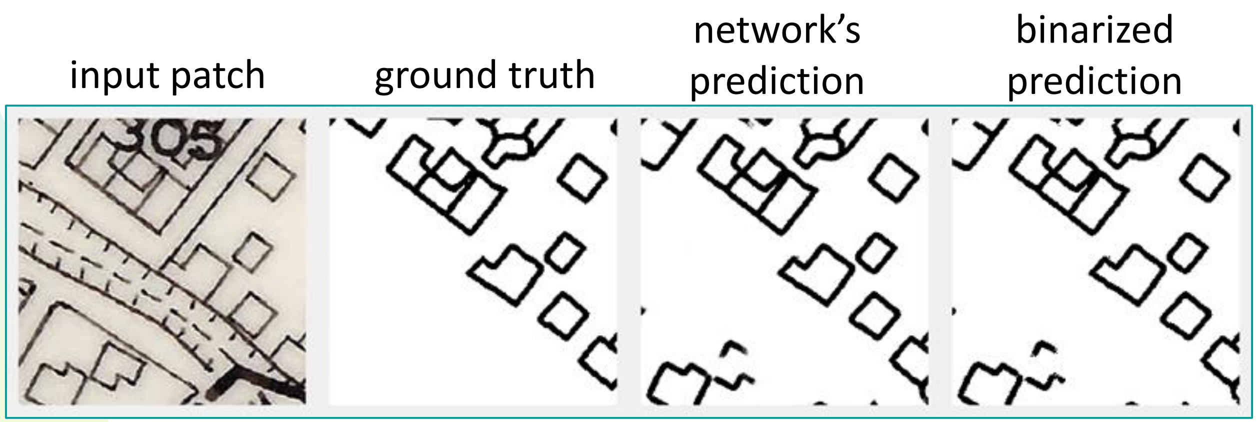

- building block number correctly removed (even if it overlaps several buildings)
- graphical representation of the riverbed is also ignored (as object of no interest).
- the buildings in the lower left part are correctly detected (even if they are missing from the ground truth!)

Buildings extraction from historical topographic maps

➢ Building **footnotes**

- Patch **size**: 64×64, 128×128 and 224×224
- Patch **sampling**: Random, Grid-Random and Grid-Grid

224x224
“Grid"

input patch

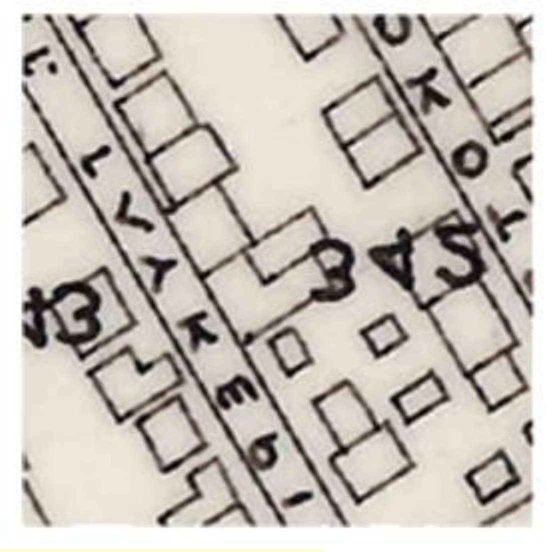

ground truth

network’s
prediction

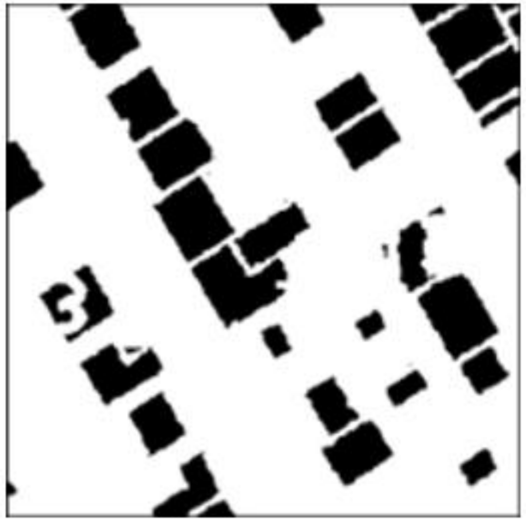

Deep learning for map generalization: Experimenting with coastline data at different map scales

Map generalization

➢ Challenges

- **Physical line** generalization (e.g., coastlines) in large-scale geospatial datasets
- From “vector-based” to “**raster-based**” generalization
- **Multi-scale maps** & **online cartographic services**
- **On-the-fly** map generalization
- …

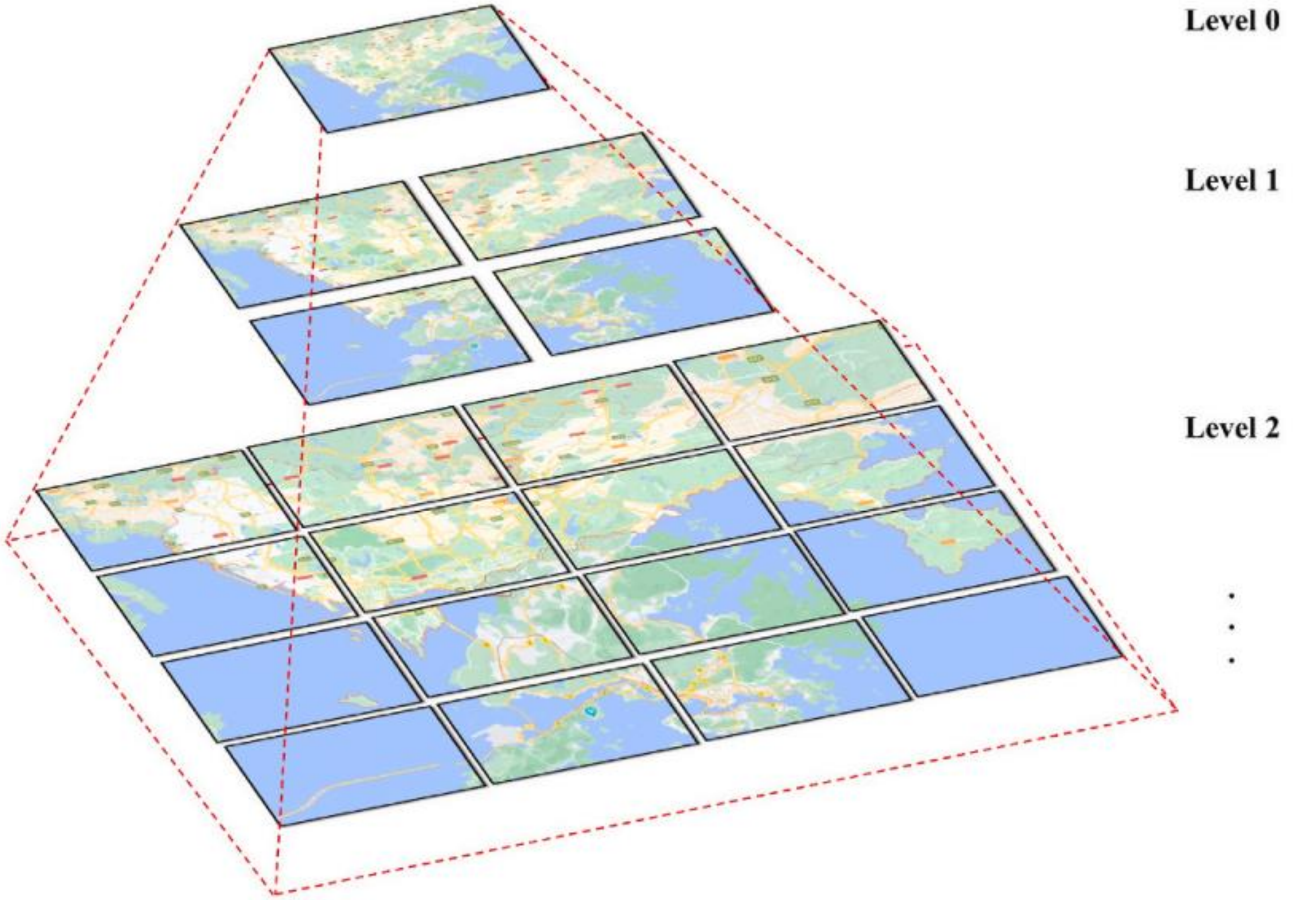

Image source: Li, G., & Li, J. (2024). An adaptive-size vector tile pyramid construction method considering spatial data distribution density characteristics. Computers & Geosciences, 184, 105537

Map generalization

➢ Training samples

- Coastline data in scales **1:1** Million, **1:3** Million and **1:10** Million
- U-Net **57** layers, **31M** learnable parameters

Larger scale image map

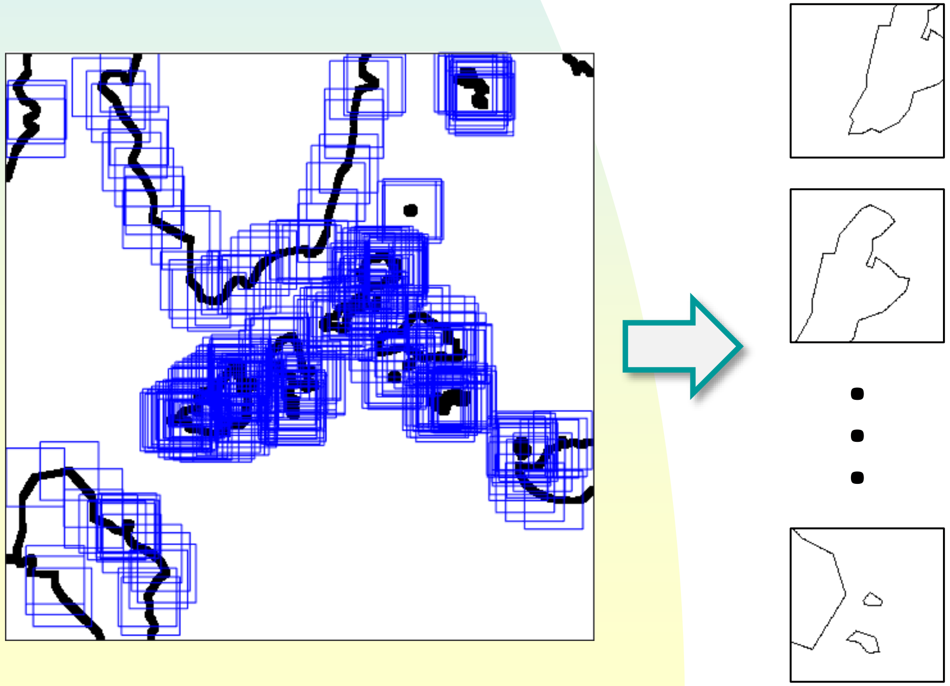

Smaller scale image map

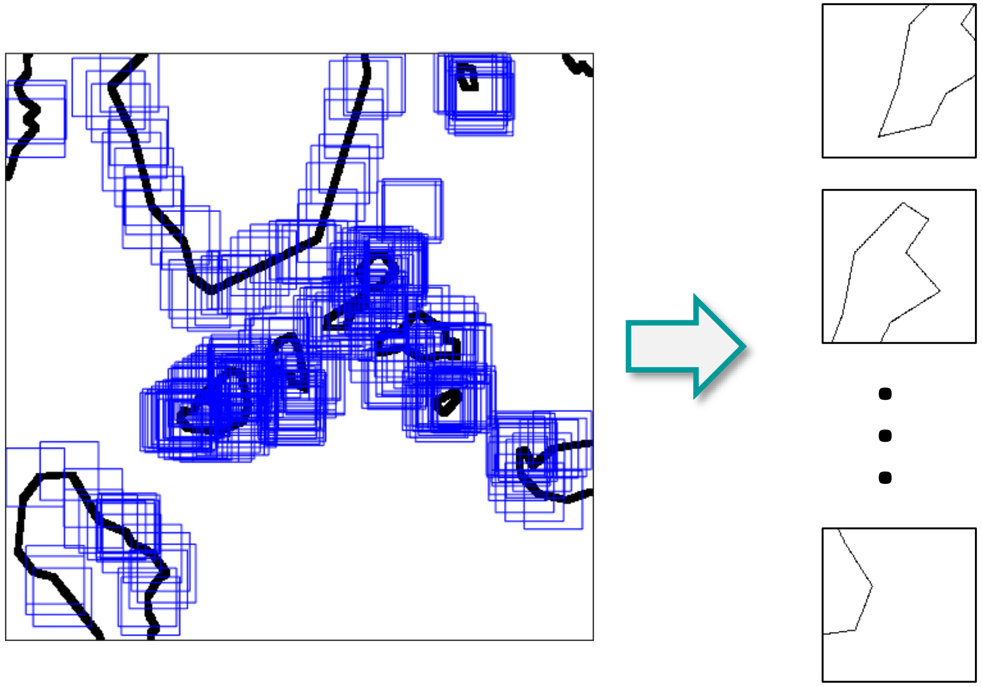

Map generalization

➢ Evaluation overview

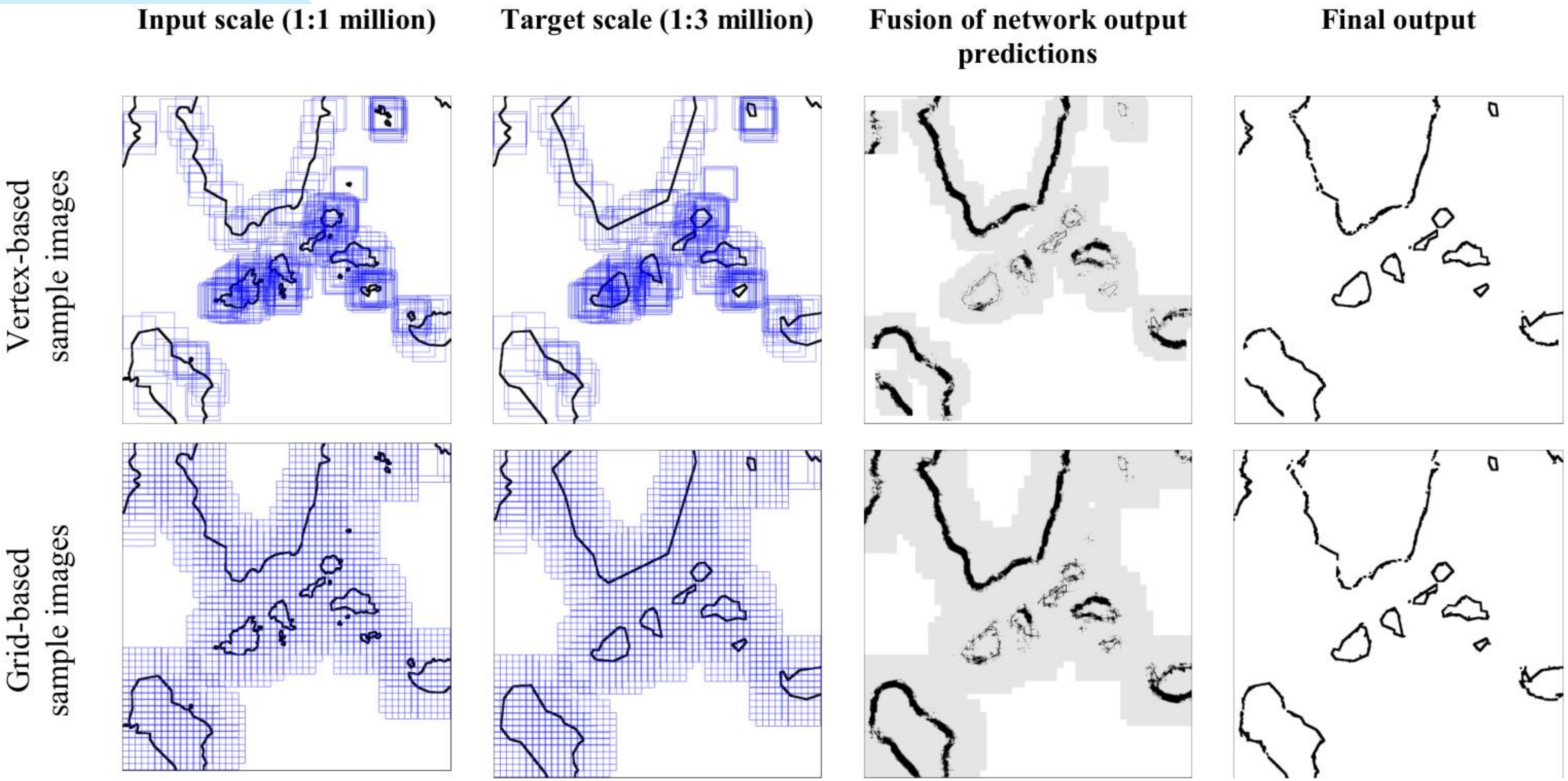

Patch **size**
128×128
64×64

Scale **pairs**
1M → 3M
3M → 10M
1M → 10M

Patch **sampling**
Grid 50×50
Grid 25×25
Vertices

Text detection on historical maps

Text detection on historical maps

➢ Challenges of Text Detection on Historical Maps

- Text can be in any orientation, any size, with variable spacing.
- Text overlaps with other text or other graphical map elements (no clear background).
- Text can be curved.

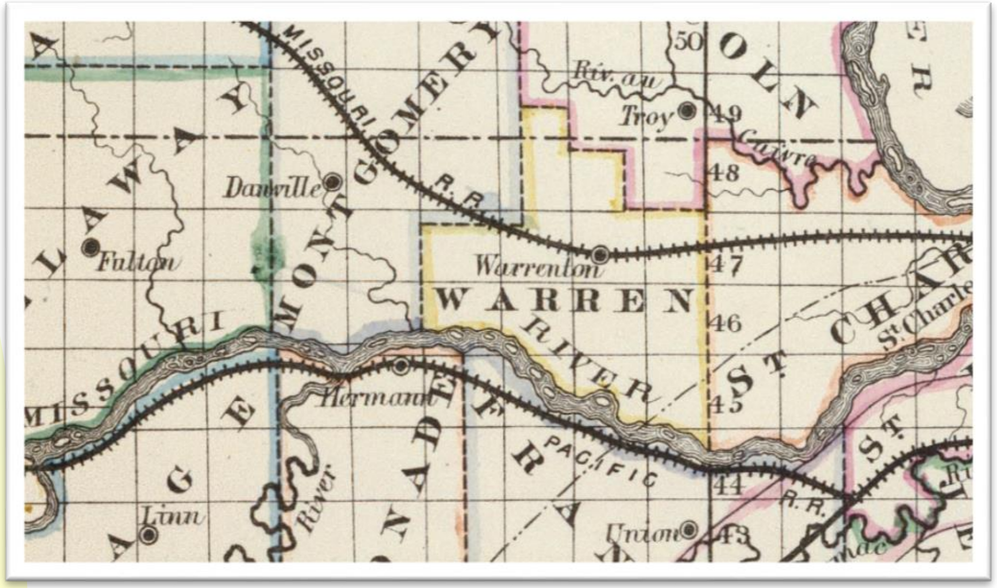

Text detection on historical maps

➢ Motivation

- The bounding box with the highest confidence score, does not always correspond to the best selection.
- There may exist other candidate boxes, also with high confidence scores, which provide more accurate predictions of the desired bounding box.

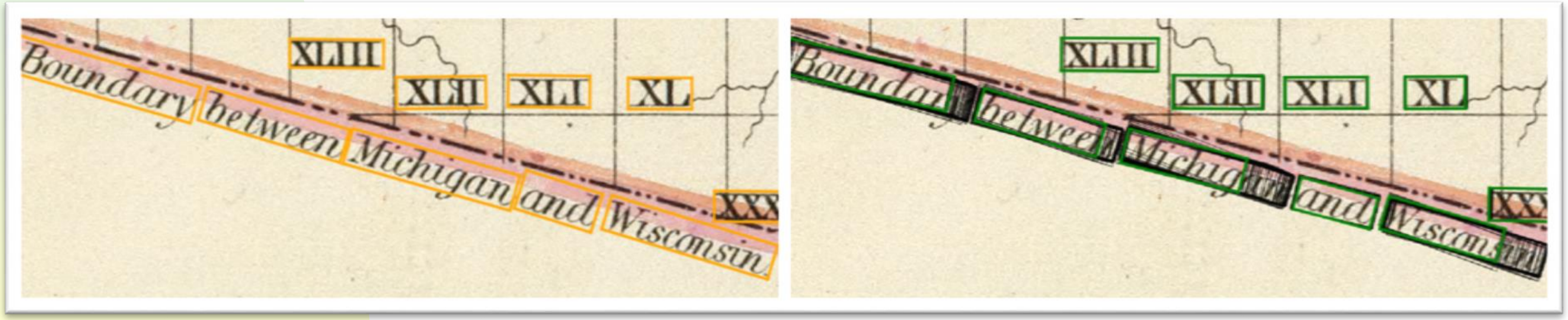

Ground Truth Bounding Boxes

Most confident prediction
Rest of highly-confident predictions

Text detection on historical maps

➢ Methodology

- Establish a post-processing step of the text detection pipeline by selecting the **best solution** among a large set of **candidate bounding boxes**, which are predicted by a deep CNN that produces dense predictions.

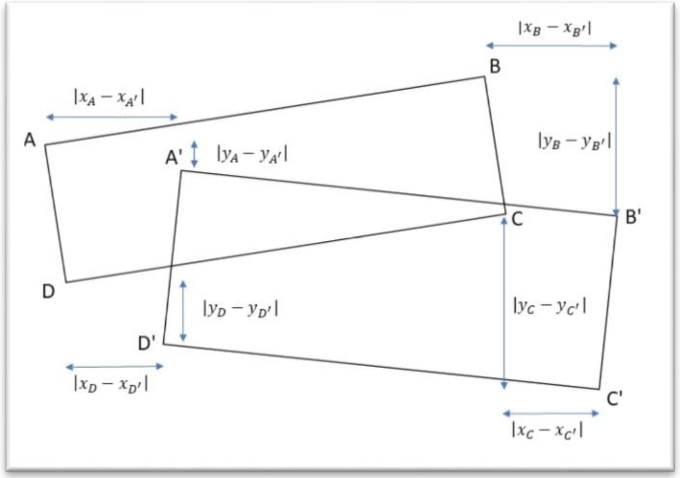

Text detection on historical maps

➢ Experimental results

- **31 historical maps from** the period **1866-1927** from the David Rumsey's Map Collection

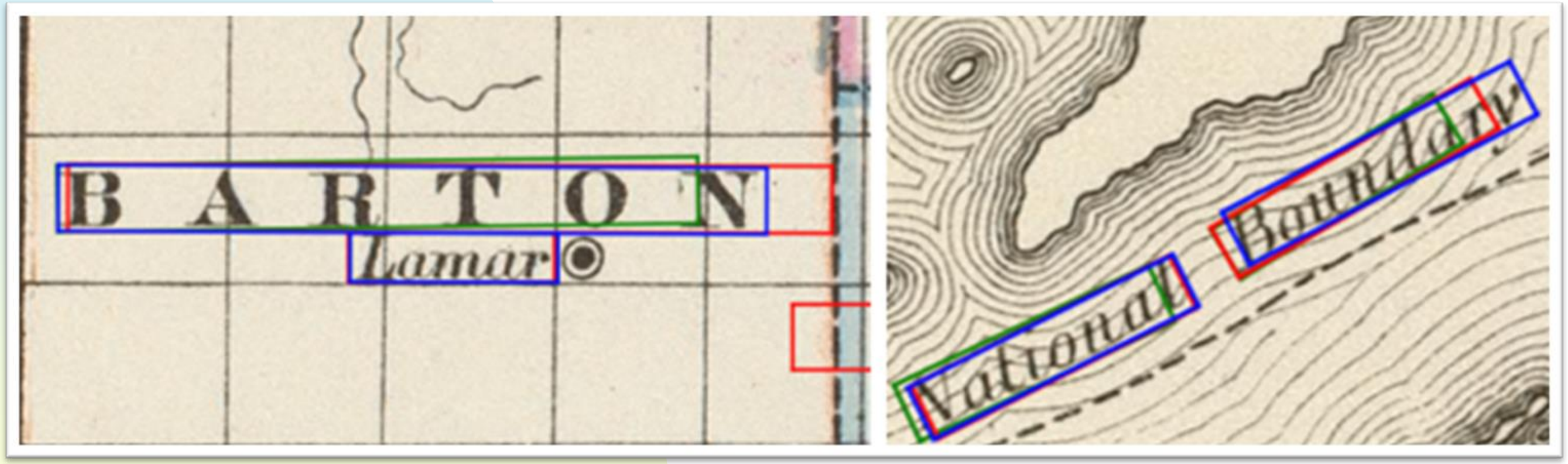

NMS, LANMS and the proposed algorithm

IoU threshold	Average Precision (%)		
	NMS	LANMS	Proposed
0.50	85.99	85.61	**87.40**
0.55	84.06	83.75	**85.89**
0.60	81.44	81.33	**84.06**
0.65	77.72	78.07	**80.90**
0.70	71.67	72.45	**75.83**
0.75	61.79	63.62	**66.96**
0.80	46.83	48.62	**52.00**
0.85	25.14	27.70	**29.47**
0.90	5.45	6.92	**7.00**
0.95	0.07	**0.11**	0.10
0.50:0.95	54.02	54.82	**56.96**

patchIT
A multipurpose patch creation tool for image processing applications

patchIT

➢ Working with patches

- Provide an integrated framework (MATLAB Toolbox) suitable for the systematic and **automatized extraction** of patches from images based on user-defined **geometrical** and **spatial** criteria.

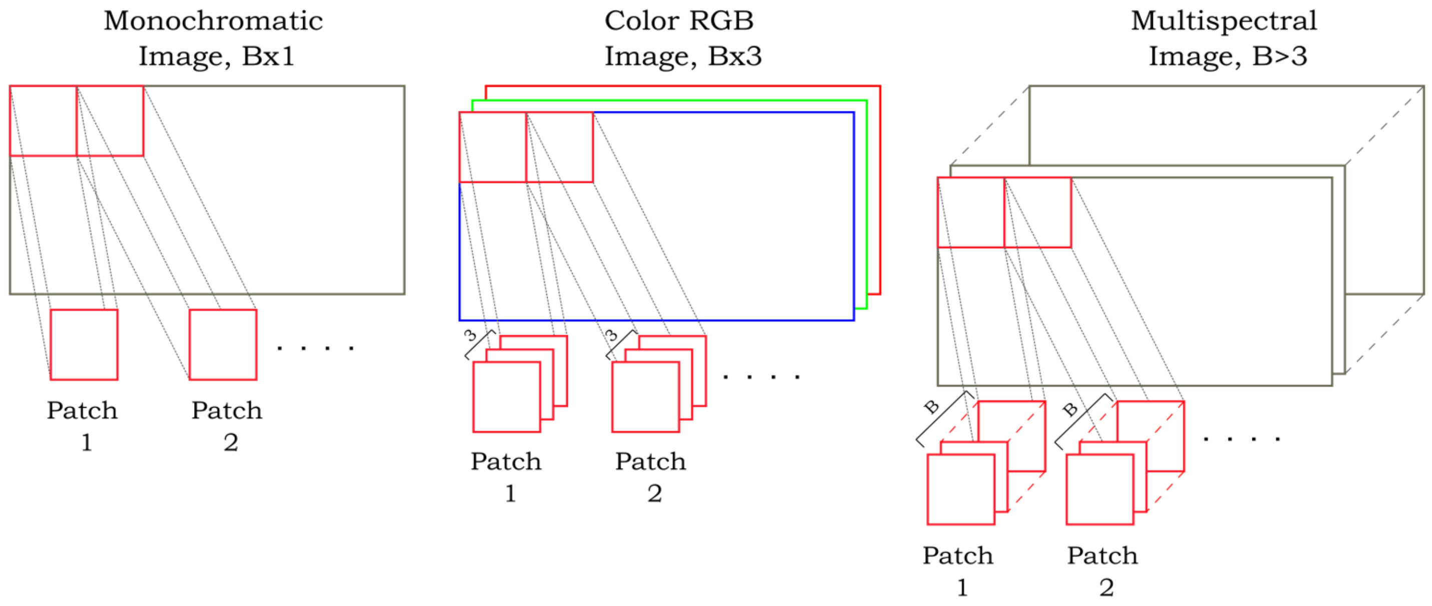

patchIT

➢ Grid-like positioning

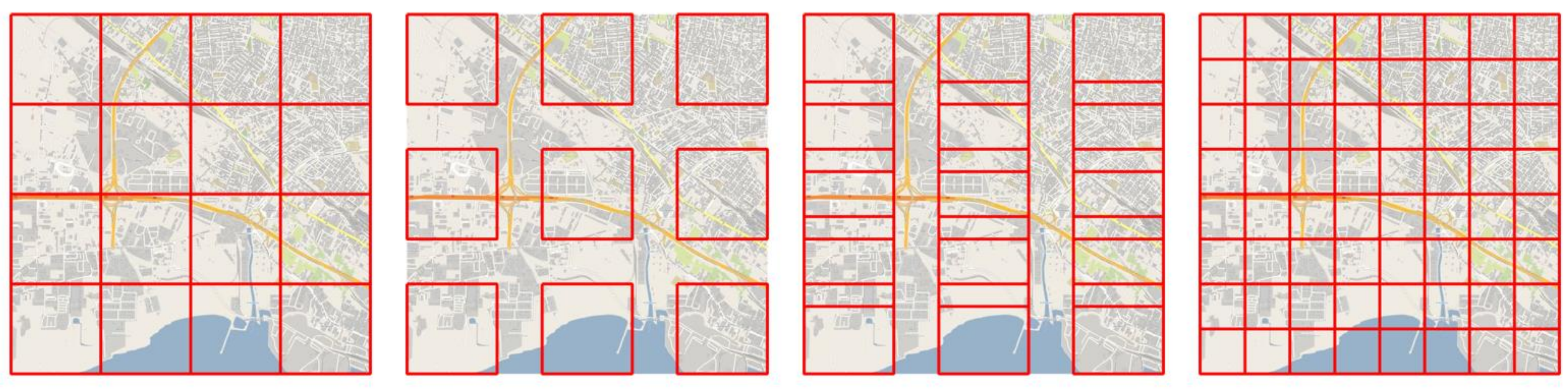

Number of patches

Stride (S_x, S_y)	Image size 1920 × 1080, Patch size $(W \times H)$: 128 × 128	32 × 32	8 × 8
(128,128)	120	135	135
(64,64)	435	510	510
(16,16)	6780	7854	8160
(4,4)	107311	124399	128851
(1,1)	1708729	1981561	2052649

Memory requirements (MB)

Stride (S_x, S_y)	Image size 1920 × 1080, Patch size $(W \times H)$: 128 × 128	32 × 32	8 × 8
(128,128)	1.875	0.132	0.008
(64,64)	6.797	0.498	0.031
(16,16)	105.938	7.670	0.498
(4,4)	1676.734	121.483	7.864
(1,1)	26698.891	1935.118	125.284

patchIT

➢ Random positioning

Determine by

i) the **number** of random patches

ii) **allowed overlap** between patches

iii) a maximum **number of attempts** to achieve a feasible solution.

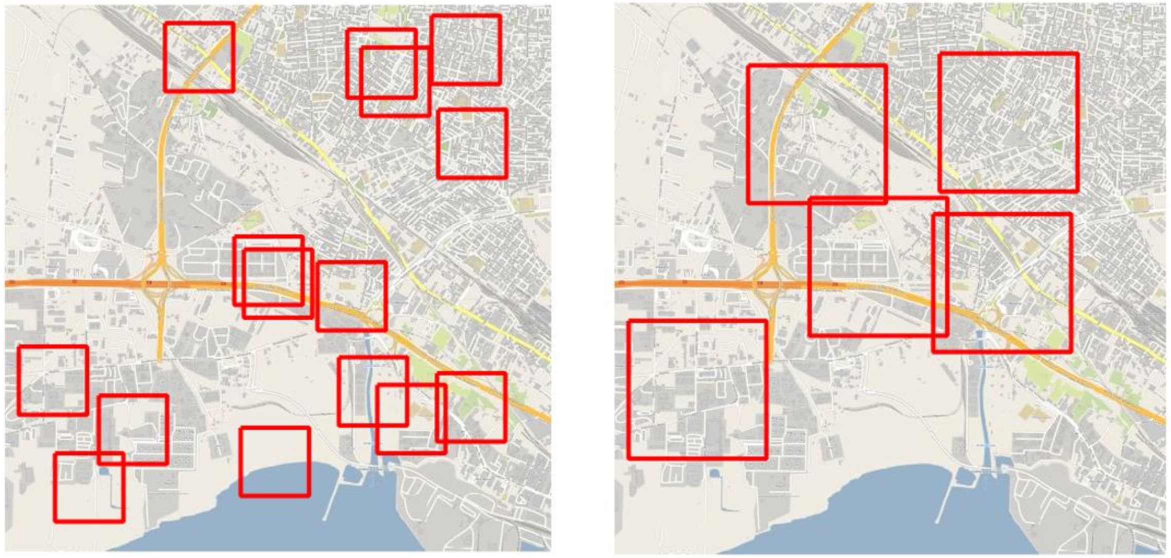

patchIT

➢ Masking

- **Sliding mode**

Exclude certain image parts from the candidate patch areas.

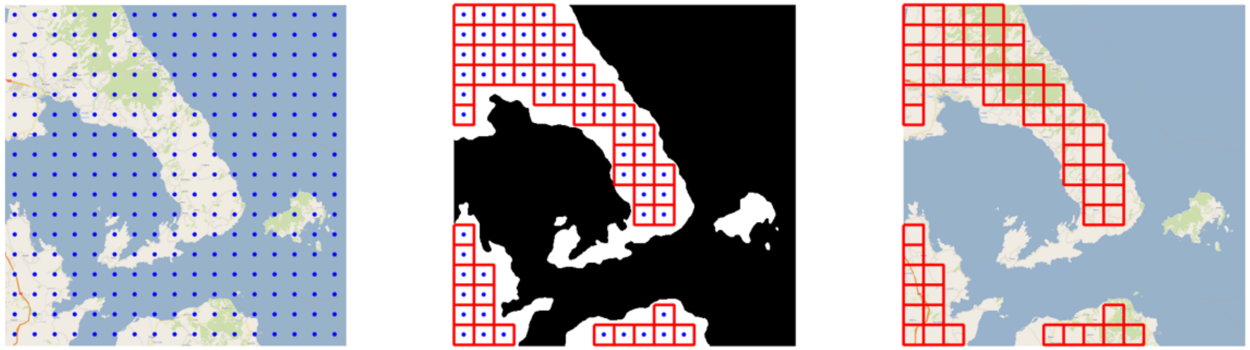

candidate patches | binary mask + patches that fit | extracted patches

- **Random mode**

A mask is considered as a **probability array** denoting favorable image areas.

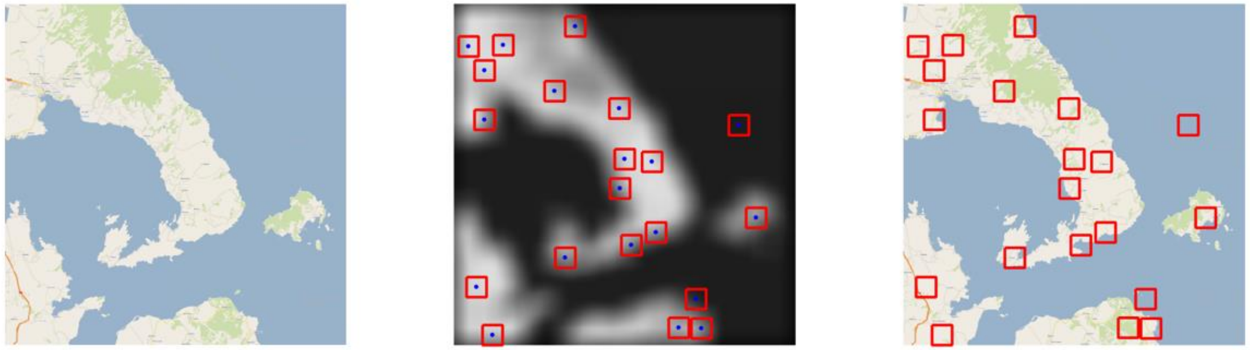

source image | probability mask + 20 patches | extracted patches

patchIT

➢ Geometric transformations

Combinational sequences of geometric transformations applied on each patch.

Operation	Resulting patch	Operation	Resulting patch
default		flip	
mirror		swap	
flip+swap (rotate 90^o clockwise)		flip+mirror (rotate 180^o)	

Patch indexing

- **Reorders** the patch intensities by user-defined patch values **indexing**, offering a deeper low-level information insight.

- Indexing modes: **default**, **mirror**, **flip**, **swap**, **spiralout**, **spiralin** (+ combinations)

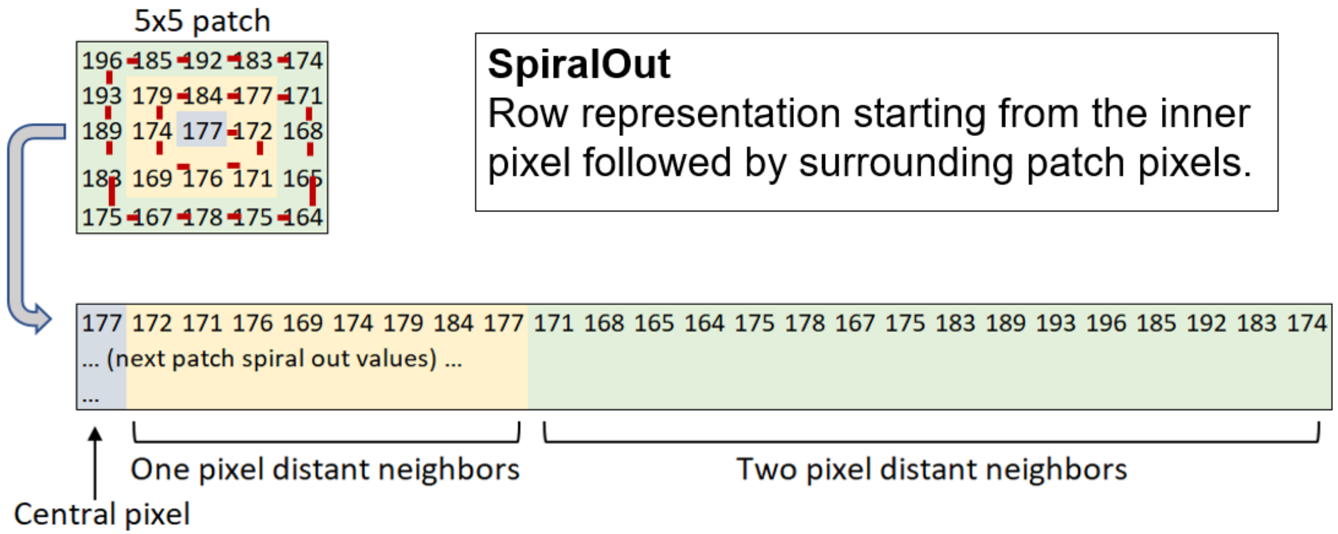

Eye-tracking and visual perception

Eye-tracking Equipment

➢ Basic specs

- **EyeLink® 1000 Plus** (SR Research Ltd)
- **Binocular** gaze data tracking
- Sample Rate of **1000Hz** (remote mode)
- Typical accuracy: **0.25° - 0.5°**

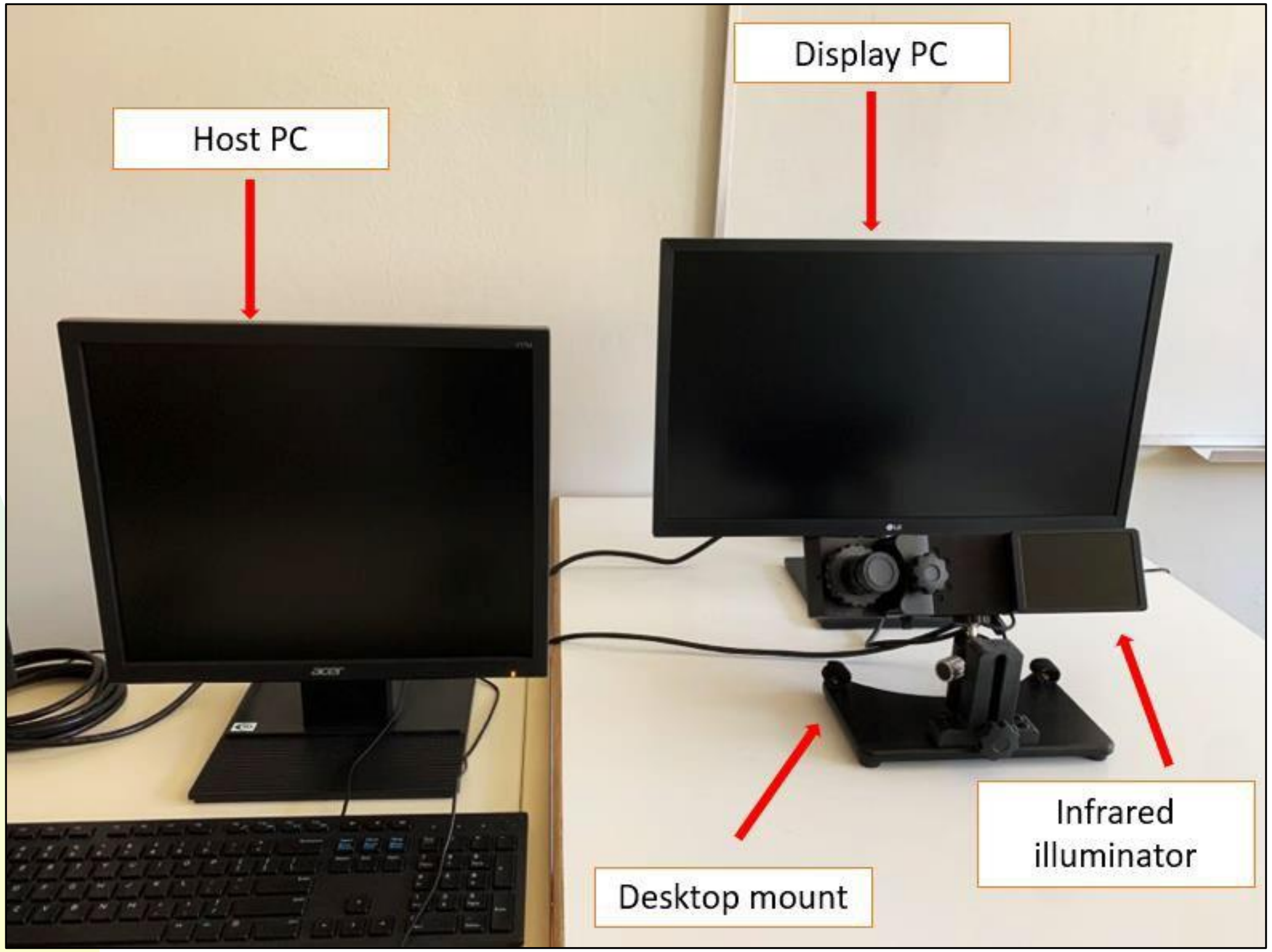

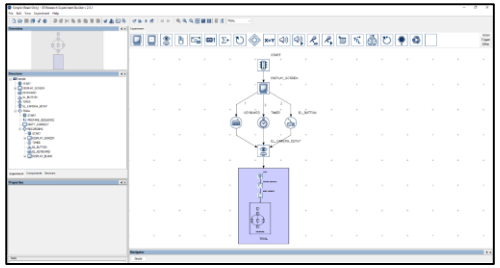

Eye-tracking Equipment: Experimental Setup

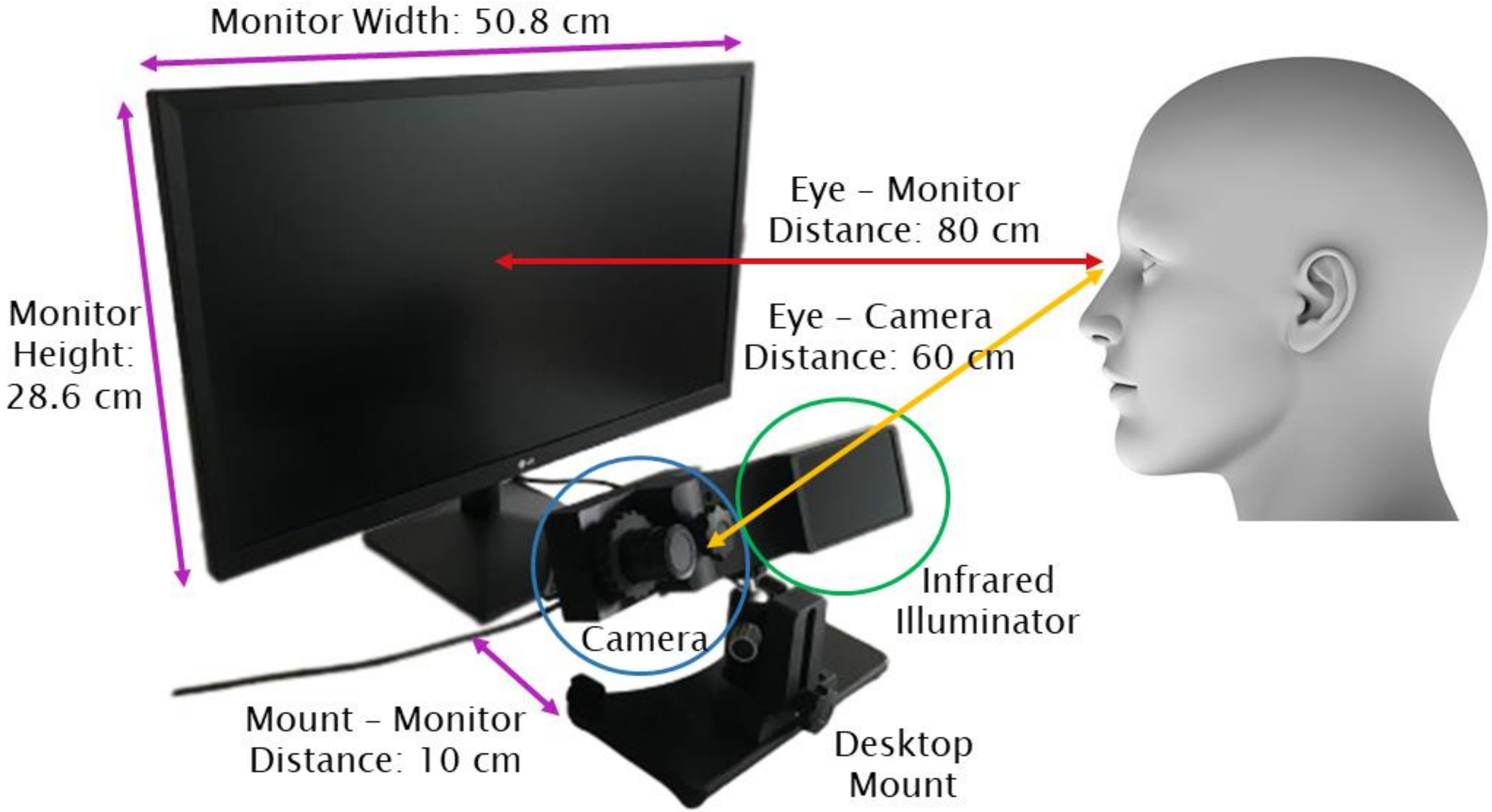

Eye-tracking Experimental Studies on Historical Maps Perception

➢ Visual stimuli

- **150 historical maps** (scanned manuscripts)
- Period: **1580-1930 a.d.**
- Resolution **1920x1080 pixels**
- **Five cartographic design styles**, characterized by different map attributes and/or elements, such as title, legend, annotation etc.
- Cartographic dataset source: David Rumsey Map Collection

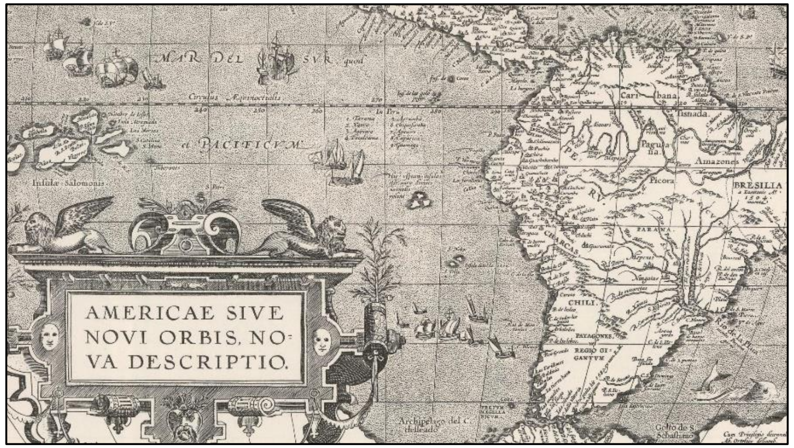

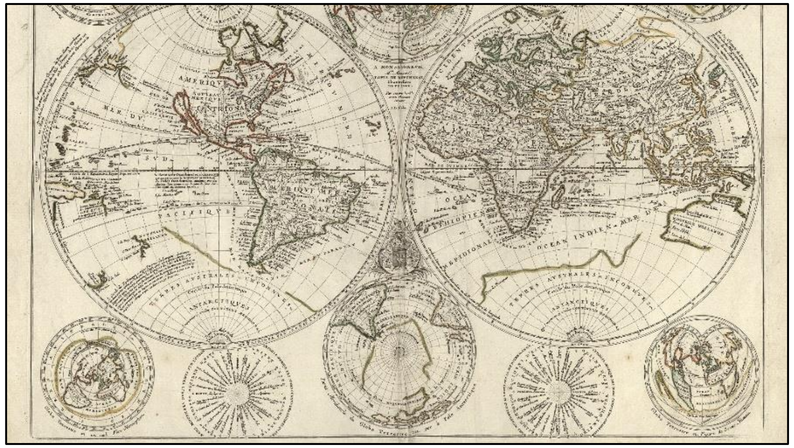

Eye-tracking Experimental Studies on Historical Maps Perception

➤ Visual stimuli

- **150 historical maps** (scanned manuscripts)
- Period: **1580-1930 a.d.**
- Resolution **1920x1080 pixels**
- **Five cartographic design styles**, characterized by different map attributes and/or elements, such as title, legend, annotation etc.
- Cartographic dataset source: David Rumsey Map Collection

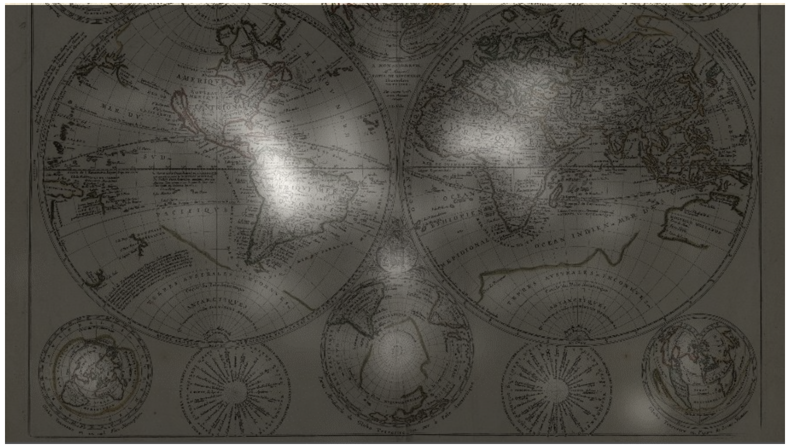

Development of Eye Movements Metrics

➢ GraphGazeD metric

- The metric can be utilized to describe both **quantitatively and qualitatively the difference between the gaze activity (pattern) on two different cartographic backgrounds** based on eye tracking data collected either under free viewing conditions or during the execution of specific map tasks.
- The GraphGazeD metric can also be implemented using **mouse tracking** data.
- The function of the metric is based on the comparison between two different **statistical grayscale heatmaps** with the same resolution and the same range of values.

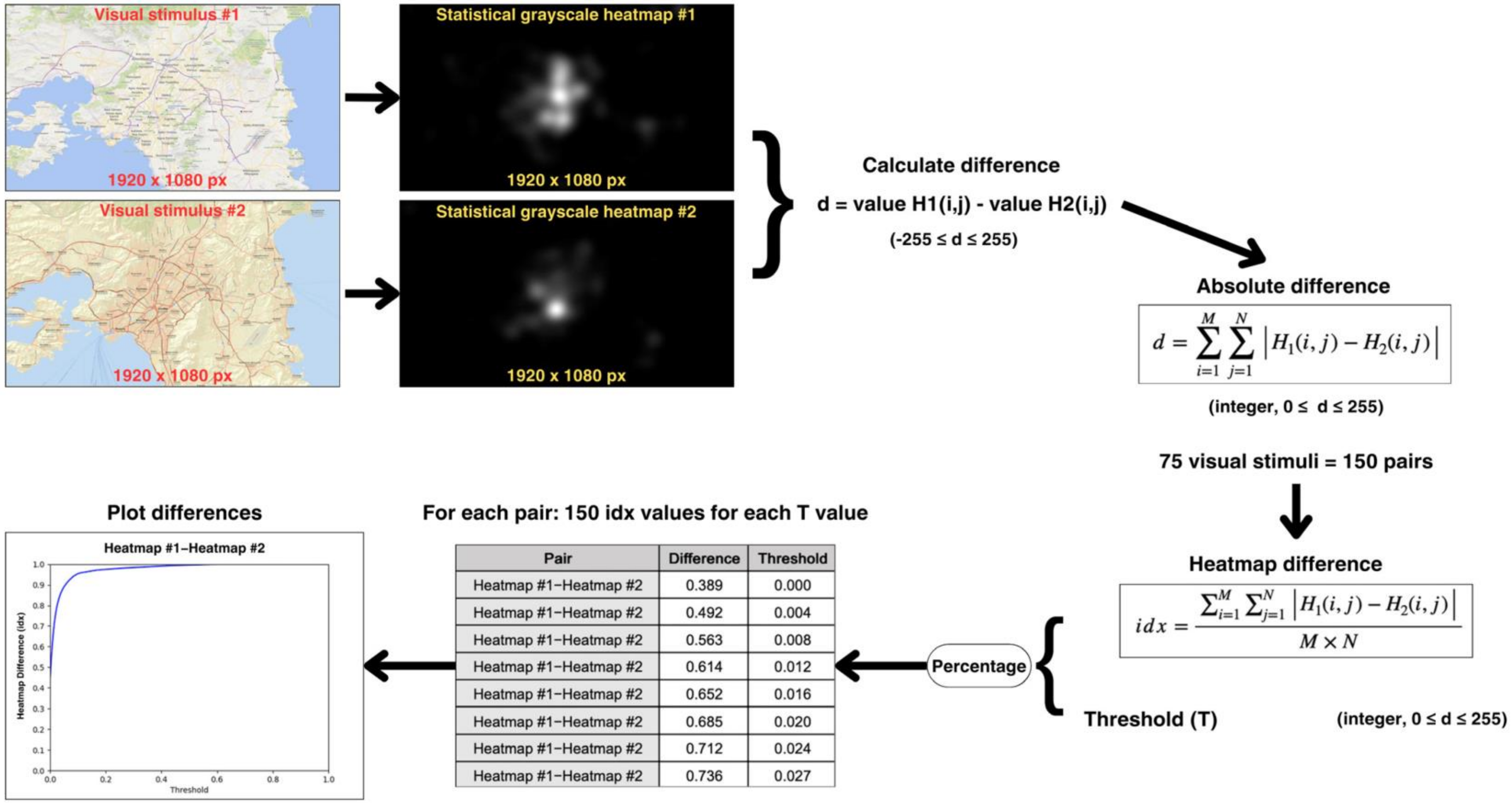

Geoportals
Map Digitization
Web Mapping

Geoportals & Spatial Data Infrastructures

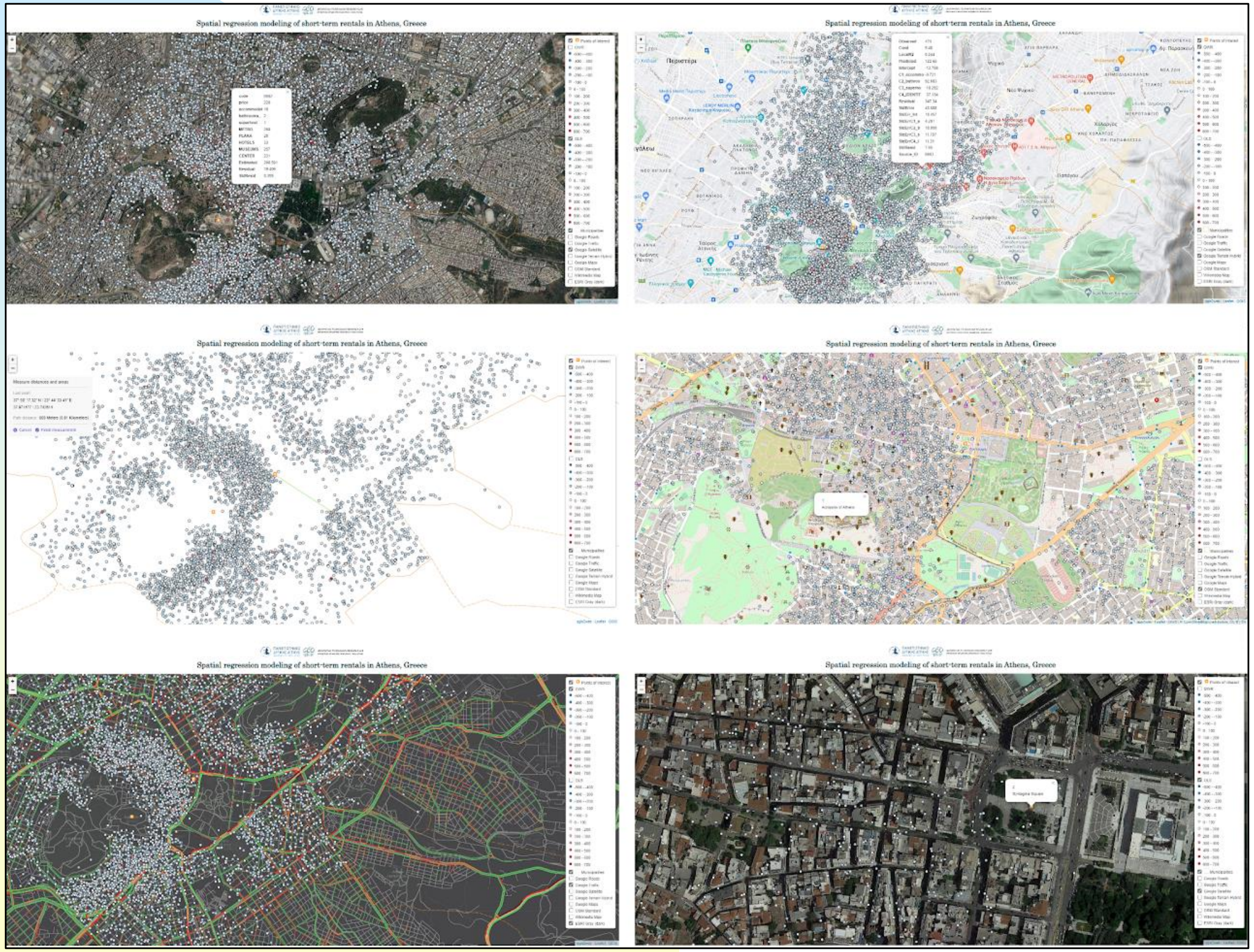

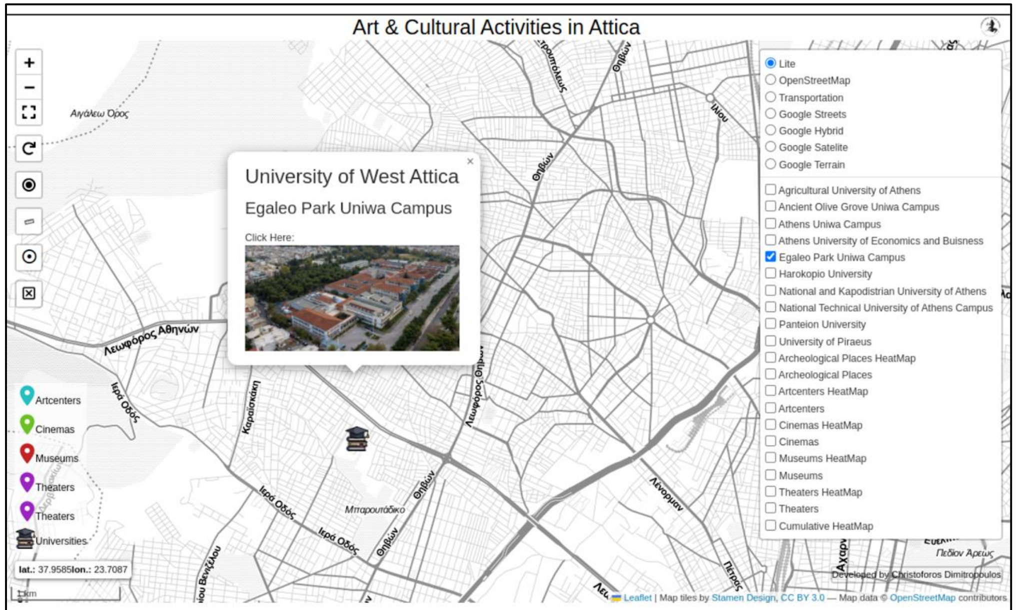

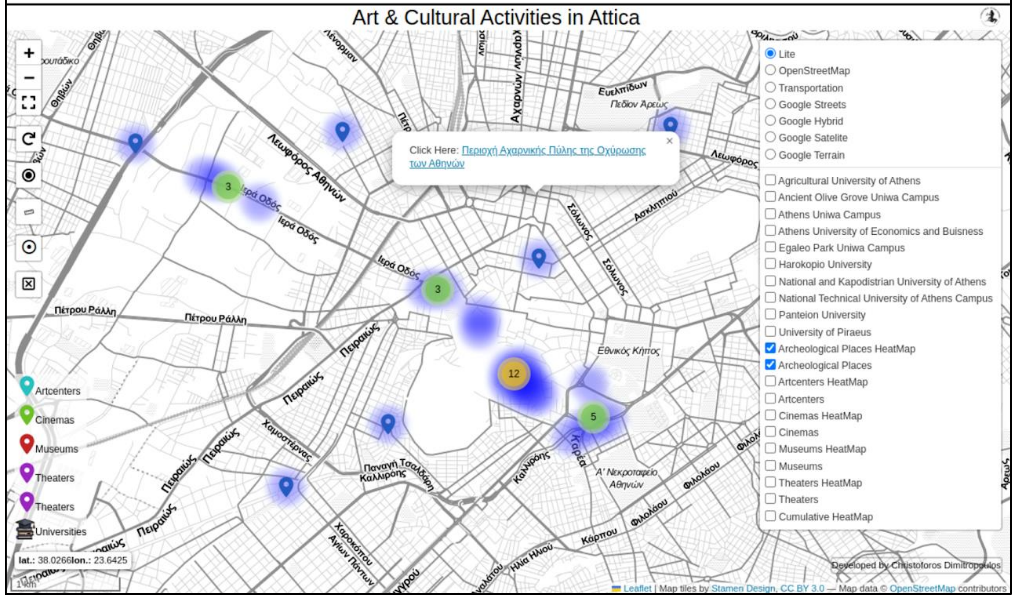

Digitizing Maps

- Kitchener's Map of Cyprus (1878-1882)

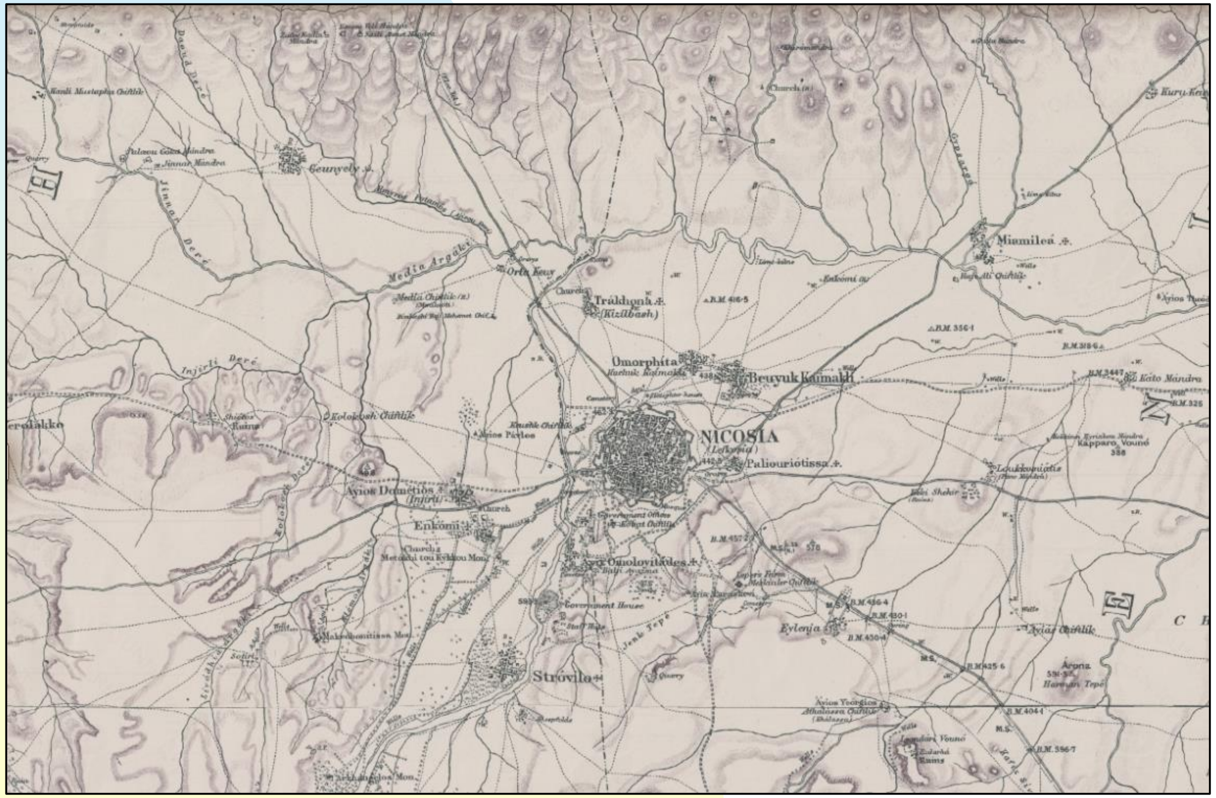

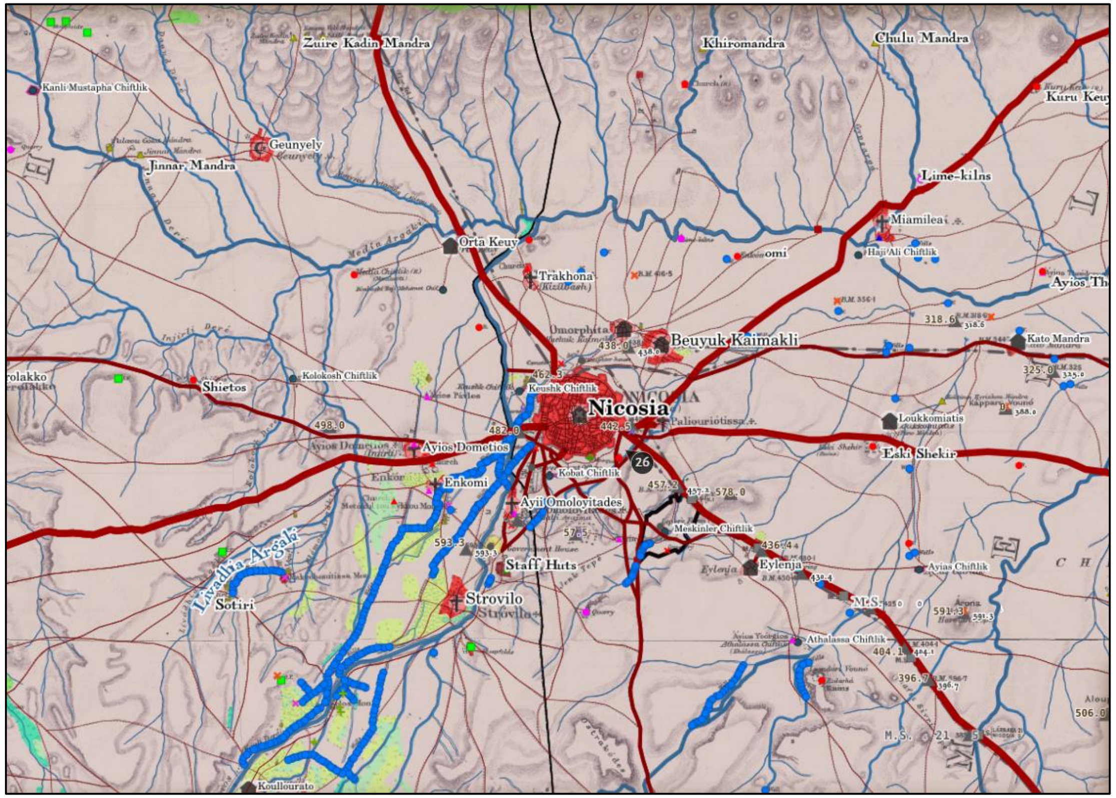

Digitizing Maps

- Kitchener’s Map of Cyprus (1878-1882)

Nicosia plan

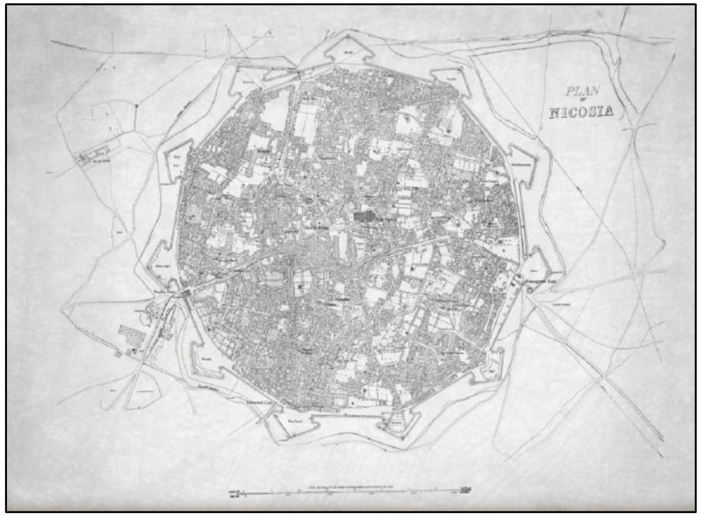

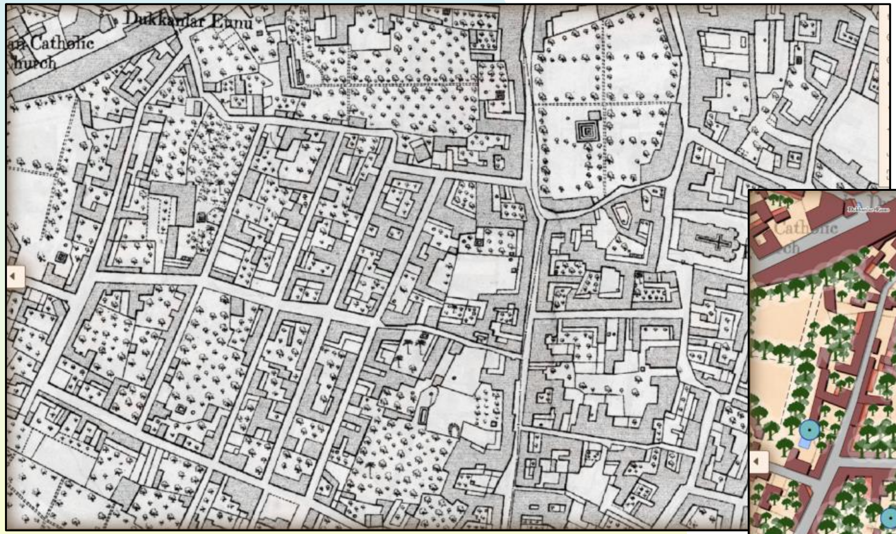

Web Mapping

- ➢ Kitchener’s Map of Cyprus (1878-1882)

https://kitchener.hua.gr/

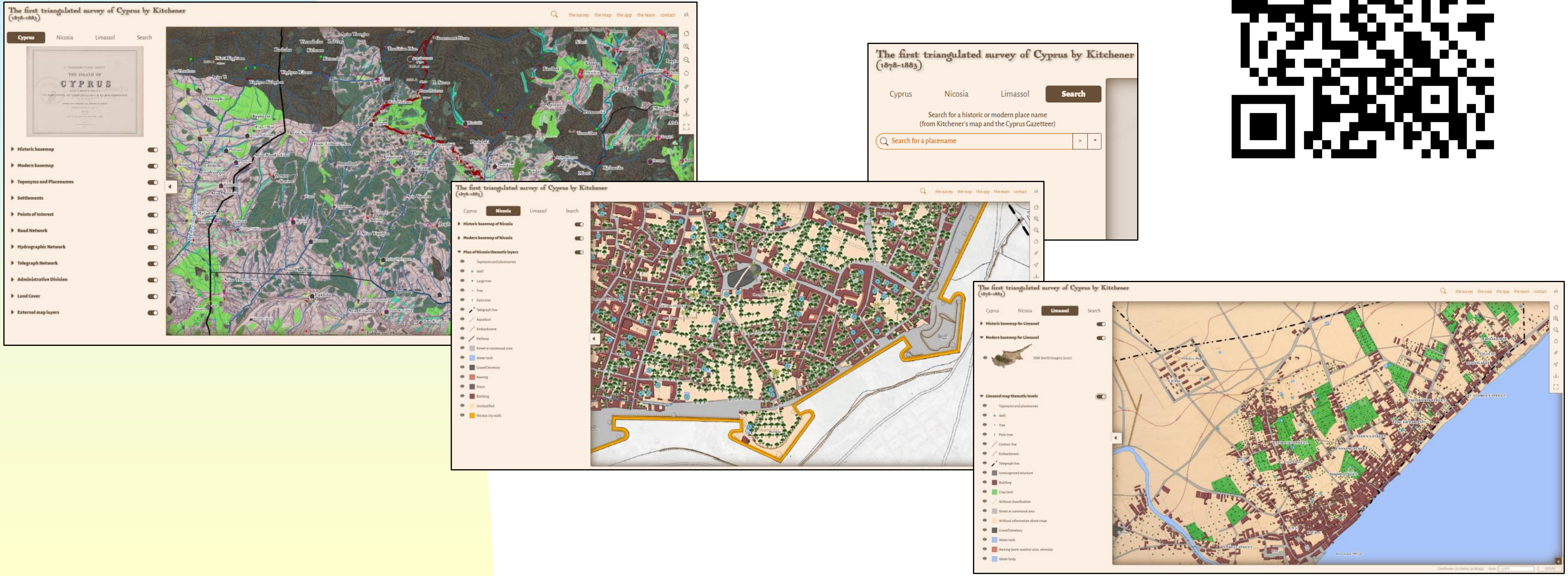

Recent publications

Xydas, C., Kesidis, A., Kalogeropoulos, K., & Tsatsaris, A. (2022). Buildings Extraction from Historical Topographic Maps via a Deep Convolution Neural Network. ***Proceedings of the 17th International Joint Conference on Computer Vision, Imaging and Computer Graphics Theory and Applications***, 485–492.

Kesidis, A. L., Krassanakis, V., Misthos, L.-M., & Merlemis, N. (2022). patchIT: A Multipurpose Patch Creation Tool for Image Processing Applications. ***Multimodal Technologies and Interaction***, 6(12), 111

Kesidis, A. L., Krassanakis, V., Merlemis, N., & Misthos, L.-M. (2022). A multipurpose patch creation tool for efficient exploration of digital cartographic products. ***European Cartographic Conference (EuroCarto2022),*** 5, 56.

Matidis, G., Gatos, B., Kesidis, A. L., & Kaddas, P. (2023). Detecting Text on Historical Maps by Selecting Best Candidates of Deep Neural Networks Output. ***International Conference for Document Analysis and Recognition*** (***ICDAR)***, 358–367.

Pinirou N., Krassanakis V., & Kesidis A.L. (2023). Examining the Visual Perception of Historical Maps via Eye Movement Analysis, ***Proceedings of the 30th Meeting of the Hellenic Society for Neuroscience (HSfN)***, 86.

Chalkias, C., Papadias, E., Vradis, C., Polykretis, C., Kalogeropoulos, K., Psarogiannis, A., & Chalkias, G. (2023). Developing and Disseminating a New Historical Geospatial Database from Kitchener's 19th Century Map of Cyprus. ***ISPRS International Journal of Geo-Information***, 12(2), 74

Viore, M., Kesidis, A. L., & Krassanakis, V. (2024). Deep learning for map generalization: Experimenting with coastline data at different map scales. ***European Cartographic Conference (EuroCarto2024)***, 7, 1–2.

Liaskos, D., & Krassanakis, V. (2024). OnMapGaze and GraphGazeD: A Gaze Dataset and a Graph-Based Metric for Modeling Visual Perception Differences in Cartographic Backgrounds Used in Online Map Services. ***Multimodal Technologies and Interaction***, 8(6), 49.

Vlachou A., Liaskos, D., & Krassanakis, V. (2024). Quantifying map user response differences between gaze and cursor activity during searching cartographic point symbols. Online User Experiments: Seeing What Map Users See without Seeing Them. ***Pre-conference Workshop European Cartographic Conference (EuroCarto2024)***.

Iliopoulou P., Krassanakis V., Misthos L.-M., & Theodoridi C. (2024). A Spatial Regression Model for Predicting Prices of Short-Term Rentals in Athens, Greece. ***ISPRS International Journal of Geo-Information***, 13(3), 63.

Papadias, E., Kalogeropoulos, K.; Polykretis, C.; Psarogiannis, A.; Chalkias, G.; Chalkias, C. (2024). Historical geospatial dataset of Cyprus from British administration maps of the 19th century, ***Data in Brief***, 57.

Dimitropoulos C., & Krassanakis V. (2023). Development of a spatial data infrastructure for art and cultural activities in Attica using free and open-source software tools (FOSS), ***Proceedings of the 16th National Cartographic Conference***, 731-742, Athens, Greece.

Liaskos, D., & Krassanakis, V. (2024). A new graph-based metric for modeling aggregated gaze behavior differences during map reading, ***European Cartographic Conference (EuroCarto2024)***, 7, 87.